



# Düzce University Journal of Science & Technology

Research Article

## Lung Nodule Detection Interface Design and Development From Computerized Tomography Images

Yasin İLHAN <sup>a\*</sup>, Arif ÖZKAN <sup>b</sup>, Bora KALAYCIOĞLU<sup>a</sup> Cantekin ÇELİKHAŞI<sup>b</sup>

<sup>a</sup> Biomedical Engineering Department, Kocaeli University, Kocaeli 41100,

<sup>b</sup> Izmit Science and Art Center, Ministry of Education, Kocaeli 41100, TURKIYE

\* Corresponding author's e-mail address: hazanyasinilhan@gmail.com

DOI: 10.29130/dubited.1417589

### ABSTRACT

Lung cancer is one of the leading diseases that cause death in the world. Early diagnosis of lung cancer is as important as its treatment. Therefore, we propose the LinkNet architecture, which is a deep learning model that will detect the location and size of nodules from the lung tomography image. The study was conducted with 110 patients and 343 nodules with nodules detected in Lung Computed Tomography (CT) Images. In the study, no public dataset was used and tomography images were obtained from the hospital. In the pre-processing stage, thresholding is made according to the lung Hounsfield Unit (HU) threshold value with the Otsu method and the lung is segmented. The XML (Extensible Markup Language) files of ROIs (Region of Interest) of the nodules previously marked by the radiologist are extracted and converted into images. Using template nodules trained with LinkNet and U-Net architectures, comparison and success percentage tables for 16 different architectures were presented. Using LinkNet, the model achieved an intersection of union (IoU) score of 69% for valid and an IoU score of 94% for the train. 274 nodule data were used in the train section and 69 nodule data were used in the validation section. Experimental results show that nodules that may be overlooked by a radiologist can be detected with CAD (Computer- Aided Design) performed and will be useful in the diagnosis of lung cancer.

**Keywords:** Lung Nodule Detection, CT Image, Otsu Thresholding, U-Net, LinkNet

## Bilgisayarlı Tomografi Görüntülerinden Akciğer Nodülü Tespit Aryüzünün Tasarımı ve Geliştirilmesi

### ÖZ

Akciğer kanseri dünyada ölüme neden olan hastalıkların başında gelmektedir. Akciğer kanserinin erken teşhisi, tedavisi kadar önemlidir. Bu nedenle akciğer tomografi görüntüsünden nodüllerin yerini ve boyutunu tespit edecek bir derin öğrenme modeli olan LinkNet mimarisinin kullanımı ile bu çalışma uygulanmıştır. Bu çalışmada, akciğer Bilgisayarlı Tomografi (BT) görüntülerinde nodül saptanan 110 görüntü ve 343 nodül modeli kullanılmıştır. Bu çalışma dahilinde herhangi bir kamuya açık veri seti kullanılmamış ve etik kurul izni dahilinde tomografi görüntüleri elde edilmiştir. Ön işleme aşamasında OTSU yöntemi ile akciğer Hounsfield Unit (HU) eşik değerine göre eşikleme yapılmış ve akciğer görüntülerine segmentasyon uygulanmıştır. Uzman radyolog tarafından işaretlenen nodüllerin ROI'lerinin (Region of Interest) XML (Extensible Markup Language) dosyaları ayıklanarak görüntülere dönüştürülmüştür. LinkNet ve U-Net mimarileri ile eğitilmiş şablon nodüller kullanılarak 16 farklı mimari için karşılaştırma ve başarı yüzdesi tabloları sunulmuştur. Model, LinkNet'i kullanarak geçerli için %69'luk birleşim (IoU) puanı ve çalışma için %94'lük bir IoU puanı elde edilmiştir. Sonuç bölümünde 274 nodül verisi, validasyon bölümünde 69 nodül verisi kullanılmıştır. Deneysel sonuçlar, radyolog tarafından gözden kaçırılacak nodüllerin yaptığımız CAD (Bilgisayar Destekli Tasarım) ile tespit edilebileceğini ve akciğer kanseri tanısında faydalı olacağını göstermektedir.

## **I. INTRODUCTION**

Lung cancer is a type of cancer that starts when abnormal cells grow in an uncontrolled way in the lungs. It is a serious health issue that can cause severe harm and death. According to World Health Organization (WHO) and major cancer research centers, lung cancer is the leading cause of cancer-related death in men and women worldwide. It is important to seek medical care early to avoid serious health effects. Treatments depend on the person's medical history and the stage of the disease. When lung nodules are detected at a treatable stage, the patient's chances of survival will be increased [1-6]. An estimated 2.1 million new cases of lung cancer were detected in the world, and 1.8 million deaths occurred due to lung cancer in 2018 [3]. According to Turkish Cancer Statistics, lung cancer is most common among Turkish men citizens. It stands out as the type of cancer and the leading cause of death. It is the fifth most common type of cancer in women [4]. The number of deaths and cases indicated shows how important early diagnosis and treatment are. Lung cancer begins when cells that consist of structurally normal lung tissue proliferate out of need and control, forming a mass (tumor) in the lung. The mass formed here primarily grows in its environment, and in later stages, it spreads to surrounding tissues or distant organs through circulation, causing damage. Early detection of lung nodules is very important in the clinical diagnosis and treatment of lung cancer. The most appropriate method used in the diagnosis of lung diseases is the Computed Tomography Imaging [5]. Computer-aided diagnosis (CA-D) system offers many supports to its users, including; Diagnosis of cancer cells from computed tomography (CT) images, their variants and predictions regarding treatment. Among the studies carried out using this method, CA-D systems created with the help of artificial intelligence technology using Computed Tomography images stand out. These CA-D systems can be automatic and semi-automatic. Considering the studies, Javaid et al. [6] in their study; firstly, contrast enhancement was performed in the preprocessing stage. Segmentation was applied with density thresholding and the external environment of the lung image was improved. After that; detection of potential nodules has been performed with K-means Clustering. Harsono et al. [7] were performed nodule detection with the "I3DR-Net" algorithm, which is called a single-stage object detector, in 1019 CT Images taken from the LIDC (The Lung Image Database Consortium) database. In the study conducted by Mukherjee et al. [8]; pulmonary nodule detection was performed with 552 high-resolution tomography images taken from Peerless Hospital. Masking was performed using Multi-Level Thresholding and segmentation of the nodules was performed with Rolling Ball Algorithm. In the study of Gupta et al. [9]; the grayscale thresholding process was performed in the first stage with 1018 CT Images taken from the LIDC database. After nodule development study was carried out with the Erosion Operation and 3D visualization of the detected nodules was designed. In the study of Kuo et al. [10]; edge optimization and noise filtration were performed with an Adaptive wiener filter in pre-processing of CT images. Lung segmentation has been performed with the Otsu method; afterward, candidate nodules were determined using the Ground Glass Opacity (GGO) feature. In the study by Zhao et al. [11]; pre-processing was performed on 800 CT images by applying thresholding, erosion, and dilation procedures. Lung was segmented with pre-processing. Candidate nodules were segmented with the U-Net algorithm. Then, nodule classification was completed with CNN (Convolutional Neural Network). In the study conducted by Aresta et al. [1], 1018 CT images taken from the LIDC database were segmented with the IW-Net algorithm. It also enables correction by analyzing two points. As can be understood from studies in the open literature, public database was used in almost all of the studies. In this study, instead of public database, actual medical images for patients with lung nodules whose diagnosis and treatment process were carried out in the hospital were used. Increasing the success of this study will help make the lung tomography images that we have studied available to the public. However, the acquisition and classification of computed tomography images are more time-consuming compared to studies with public database. In addition, while comparisons were made with a single architectural structure in all of the studies carried out, 16 different models were compared in this study. Hyperparameters at the U-Net and LinkNet

structure are adapted to the nodule segmentation process. U-Net and LinkNet algorithms used and fast processing capacity despite the high number of parameters are among other advantageous conditions.

Detection of nodules by radiological examinations requires superior clinical knowledge and is time-consuming, and the diagnosis process becomes more difficult as the shape and density of the nodules change [1-5]. The system design that automatically detects the nodule will make this situation advantageous for both patients and radiologists.

The purpose of this study; To assist the diagnosis process by detecting nodules with the fully automatic CA-D system, without being dependent on radiologists in the subsequent procedures of lung tomography images. Thus, nodules that the physician missed during the examination will be detected and medical errors that occur during the diagnosis process will be prevented.

## II. METHODOLOGY

The study consists of four main processes; segmentation of the lung parenchyma, marking of the nodules by a radiologist, taking images of the nodules, and detecting the nodules. In the first step of this study, lung segmentation is performed and then in the the segmentation process, the nodules are marked by the radiologist. The last step, in order to detect the nodules, which is the main purpose of the project, only the segmentation of the relevant area including the lung is performed. The Computed Tomography images used in this study are not public data sets but are the data of 110 patients with nodules detected in the lung tomography images of the Ministry of Health Kocaeli Izmit Seka State Hospital. In the beginning, tomography images of 300 patients in total were obtained from this hospital with the permission of the ethics committee. However, in patients whose cancer tissue was clearly evident in tomography images, nodules were detected by chest diseases specialists, but no nodules were found, and respiratory and motion artifacts that occurred on tomography were not included in the study. A total of 343 nodules belonging to 110 patients were identified by the radiologist. 274 nodules were used as training data and 69 nodules as validation data. This study was performed in line with the principles of the Declaration of Helsinki. Approval was granted by the Ethics Committee of Kocaeli University. (Approval Date: 16.11.2020 / Approval Number: 78754) Overview of the proposed lung nodule detection framework is given in Figure 1.

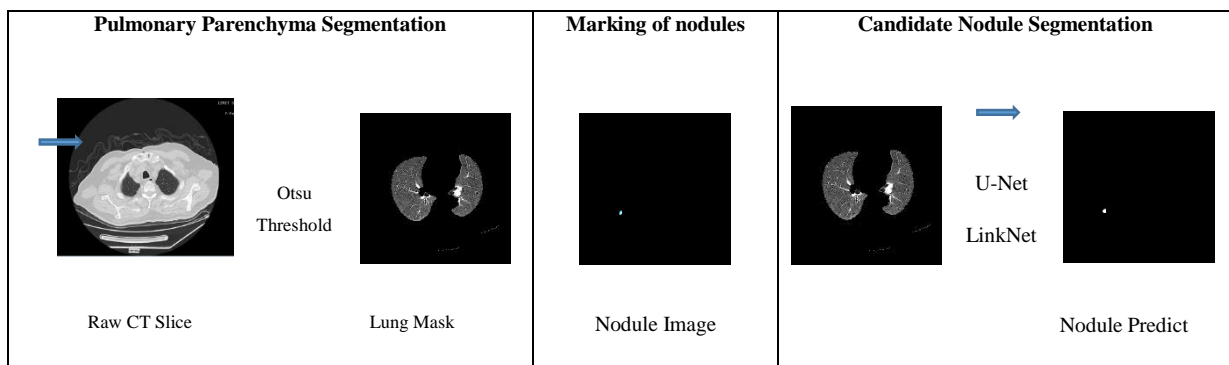


*Figure 1. Overview of proposed lung nodule detection framework*

### A. PULMONARY PARENCHYMA SEGMENTATION

At this stage, only the area containing the lung border was segmented and the area outside the lung border was removed. This process was performed by thresholding using the HU values in the Computer Tomography Images. The values measured and digitized by the detectors are converted into X-ray capture values of each voxel by computers. This is done according to a scale that assumes the X-ray

absorption value of water to be 0, with one end being  $-1000$  and the other end being  $+3095$ . The scale used is called the Hounsfield Unit, and the numbers on this scale are called CT Units or HU Units, after the British Physicist Hounsfield who was one of the developers of the method [2]. In HU, each value represents a texture. For example, the value  $-1000$  represents air, while the range of values  $+400 - +1000$  represents bone tissue. The range of  $600 - 700$  is the range of HU values for the lung [12]. To segment the lung, the part containing the lung area is taken by adjusting the  $-1024$  HU value below 0, and the other parts are cut and discarded. 0 and above  $-1000$  HU values of air and bone tissue were not taken into account and lung HU value range was used as the threshold scale. The Otsu method was used in the study for thresholding.

Otsu algorithm is the concept of binary thresholding, the parts of an array (image matrix) below a certain threshold value are 0; it is an algorithm that is used to create a binary image by making the above parts as 1 [12]. After thresholding, images containing only the borders of the lung will be obtained. Segmented lung image with the Otsu method is given by Figure 2.

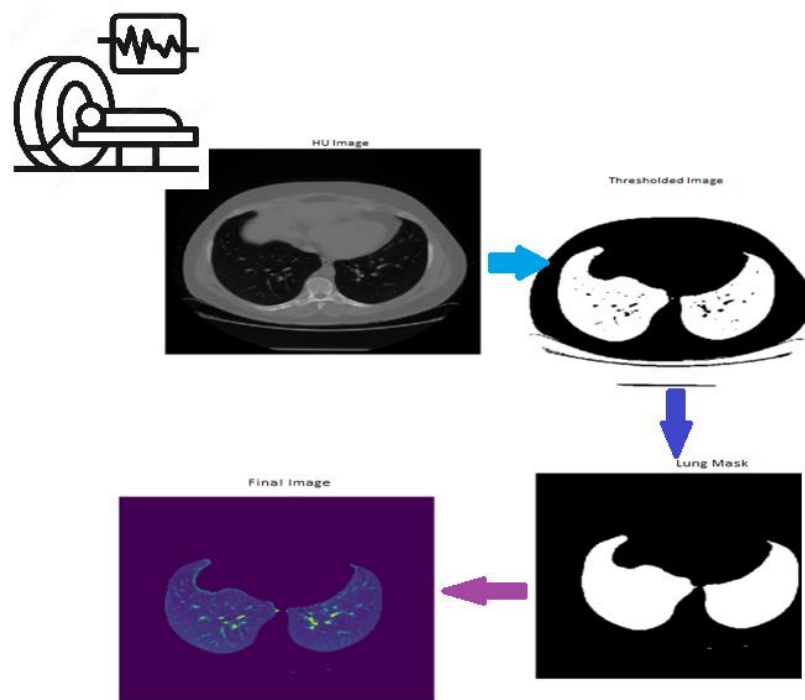


*Figure 2. Lung parenchyma segmentation structure*

## **B. MARKING OF NODULES**

The locations of the nodules are marked by the radiologist from the tomography images of 110 patients with nodules. Computed Tomography images with nodules are marked by the radiologist using the Osirix program. Numerical data regarding the positions of the nodules are exported as an XML file to enable processing. Osirix software performs operations such as navigation and processing of Multi-modal and multi-dimensional images with impressive speed. The contents maintained in this way provide the opportunity to proceed easily during the transactions without the need for additional requirements. The software was developed in Objective-C, an object-oriented programming language, using a Macintosh platform under the MacOS X operating system. It also takes advantage of the high-speed and optimized 3D graphics capabilities of the OpenGL graphics development interface commonly used for computer games. In the design of the software, its user-friendly feature, which enables navigating between large image data sets and performing complex operations, has been prioritized [13]. The reason why the Osirix program is preferred for marking nodules due to the specified requirements

is that the marked ROI regions can be converted into numerical data and exported. After the nodules are marked on the tomography images determined in the Osirix software and their coordinates are determined, the process is completed by exporting the definitions of the ROI regions as an XML file containing the indexes.

### C. CREATING NODULE IMAGES

It is the stage in which the images of the nodules for which numerical position data have been created by marking them by the radiologist are created. The numerical values of the nodule in the XML files (Figure 3) are matched with the image in that section and the patient name in which section of the computed tomography image of the patient. Looking inside the XML files, there are libraries for each nodule and the position values in the x and y coordinate plane of the marked nodule. Nodule masks were created by setting the fields with the position values obtained from the XML file to 1 through a matrix with the created 512x512 field values of 0. These nodule masks will be used for matching segmented lung images.

When looking at the XML file, the total section in the patient's tomography image, the number of the processed section in the image, the patient's number, the length and width values of the image, the number of ROIs, the ROI method, etc. information is included. The following data is location data and includes area information. Nodule masks are created using this data. Figure 4 shows sample nodule masks in different shapes and positions belonging to different patients used in this study.

```
<?xml version="1.0" encoding="UTF-8"?>
<!DOCTYPE plist SYSTEM "http://www.apple.com/DTDs/PropertyList-1.0.dtd" PUBLIC "-//Apple//DTD PLIST 1.0//EN"
- <plist version="1.0">
- <dict>
- <key>Images</key>
- <array>
- <dict>
<key>ImageHeight</key>
<integer>512</integer>
<key>ImageIndex</key>
<integer>50</integer>
<key>ImageTotalNum</key>
<integer>88</integer>
<key>ImageWidth</key>
<integer>512</integer>
<key>NumberOfROIs</key>
<integer>1</integer>
<key>ROIs</key>
<array>
- <dict>
<key>AreaCm2</key>
<real>0.064369224011898041</real>
<key>AreaPix2</key>
<real>9</real>
<key>Center</key>
<string>(-140.447083, 30.816563, -193.500000)</string>
<key>Dev</key>
<real>225.27650451660156</real>
<key>IndexInImage</key>
<integer>0</integer>
<key>LengthCm</key>
<real>0.0</real>
<key>LengthPix</key>
<real>4.7784277633476262e-43</real>
<key>Max</key>
<real>87</real>
<key>Mean</key>
<real>-229.22222900390625</real>
<key>Min</key>
<real>-592</real>
<key>Name</key>
<string>BöLge</string>
<key>NumberOfPoints</key>
<integer>12</integer>
<key>Point_mm</key>
<array>
<string>(-142.135178, 29.970861, -193.500000)</string>
<string>(-142.135178, 30.816563, -193.500000)</string>
<string>(-142.135178, 31.662266, -193.500000)</string>
<string>(-141.292786, 32.504665, -193.500000)</string>
<string>(-140.447083, 32.504665, -193.500000)</string>
<string>(-139.601379, 32.504665, -193.500000)</string>
<string>(-138.759003, 31.662266, -193.500000)</string>
<string>(-138.759003, 30.816563, -193.500000)</string>
<string>(-138.759003, 29.970861, -193.500000)</string>
<string>(-139.601379, 29.128462, -193.500000)</string>
<string>(-140.447083, 29.128462, -193.500000)</string>
<string>(-141.292786, 29.128462, -193.500000)</string>
</array>
</dict>
</array>
</dict>
</plist>

</array>
<key>Point_px</key>
<array>
<string>(120.003922, 304.000000)</string>
<string>(120.003922, 305.000000)</string>
<string>(120.003922, 306.000000)</string>
<string>(121.000000, 306.996078)</string>
<string>(122.000000, 306.996078)</string>
<string>(123.000000, 306.996078)</string>
<string>(123.996078, 306.000000)</string>
<string>(123.996078, 305.000000)</string>
<string>(123.996078, 304.000000)</string>
<string>(123.000000, 303.003922)</string>
<string>(122.000000, 303.003922)</string>
<string>(121.000000, 303.003922)</string>
</array>
<key>Point_value</key>
<array>
<real>5</real>
<real>87</real>
<real>-365</real>
<real>-82</real>
<real>18</real>
<real>-400</real>
<real>-336</real>
<real>-398</real>
<real>-592</real>
</array>
<key>RadiusHeightCM</key>
<real>0.0</real>
<key>RadiusHeightPIX</key>
<real>0.0</real>
<key>RadiusWidthCM</key>
<real>0.0</real>
<key>RadiusWidthPIX</key>
<real>0.0</real>
<key>SOPInstanceUID</key>
<string>1.2.840.113619.2.428.3.688540491.218.1579681712.393.51</string>
<key>SeriesInstanceUID</key>
<string>1.2.840.113619.2.428.3.688540491.218.1579681712.124.3</string>
<key>StudyInstanceUID</key>
<string>1.2.840.113619.2.428.3.688540491.218.1579681712.115</string>
<key>Total</key>
<real>-2063</real>
<key>Type</key>
<integer>20</integer>
</array>
</dict>
</plist>
```

Figure 3. XML example of created nodule mask

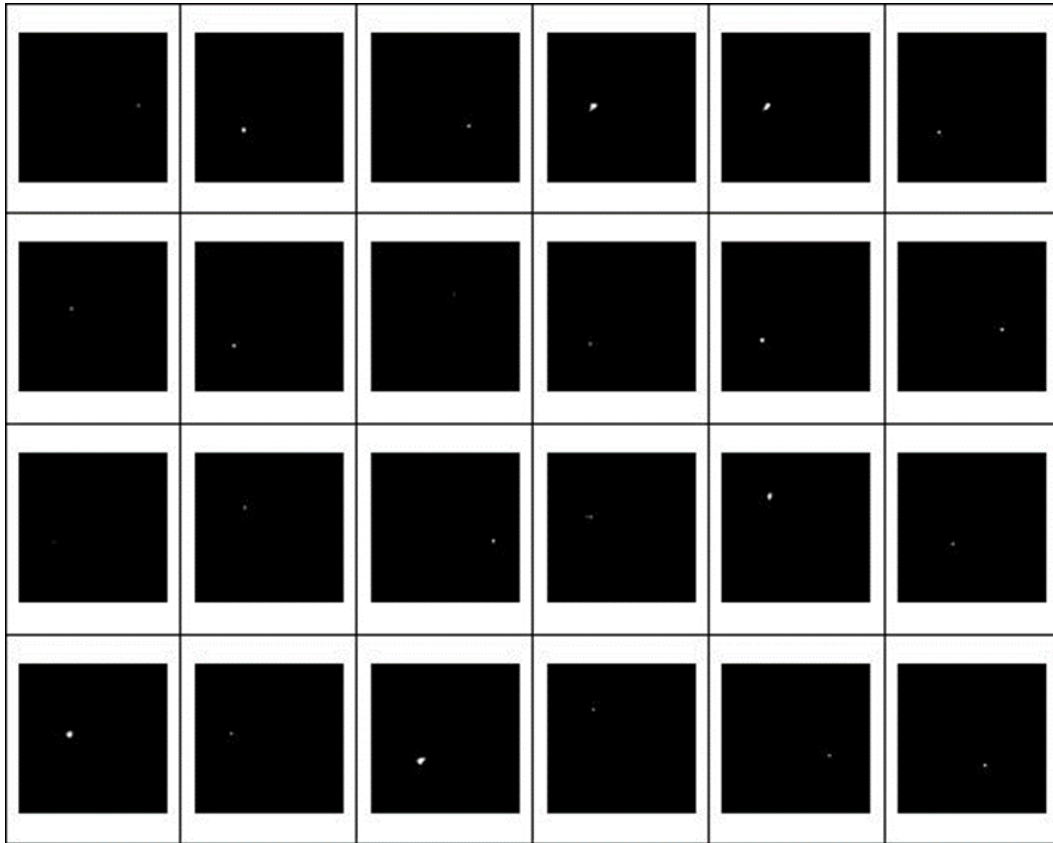


*Figure 4. Images of marked nodules.*

#### **D. CANDIDATE NODULE SEGMENTATION**

It is the stage where the created nodule masks are searched in segmented lung tomography images and matching is performed. When the nodule masks match the true nodules, they are segmented from the masked lung. The segmentation of the nodules was carried out using the LinkNet and U-Net architecture. This studies' goal was to work on multiple models to find the model with the highest success. In the study, the highest success was seen in the LinkNet model when compared with other models. U-Net is a kind of CNN approach. It was introduced by Olaf Ronneberger, Phillip Fische, and Thomas Brox in 2015 [14]. Their main aim was to perform better segmentation of medical images. It is named so because the shape of the model resembles the letter U. U-Net method is more successful than other conventional models, even with limited dataset images [14]. LinkNet architecture used series of the decoder and encoder blocks for breaking down the image and make it up again before passing it towards a final convolutional layer. For real-time segmentation, the number of parameters should be minimized for this structure of the network was designed. LinkNet is a relatively easy-working network with around 11.5 million parameters different from difficult networks like VGG which has 10x more workload [15]. For the reasons stated, the use of U-Net and LinkNet algorithm provided advantages in the project. It has been chosen because the highest success is on the LinkNet. We recommend the LinkNet algorithm because we achieved the highest success in this study. The architecture of the LinkNet is given in Figure

5 (a), convolutional modules in encoder-block are given in Figure 5(b) and convolutional modules in decoder-block are given in Figure 5(c) [15].

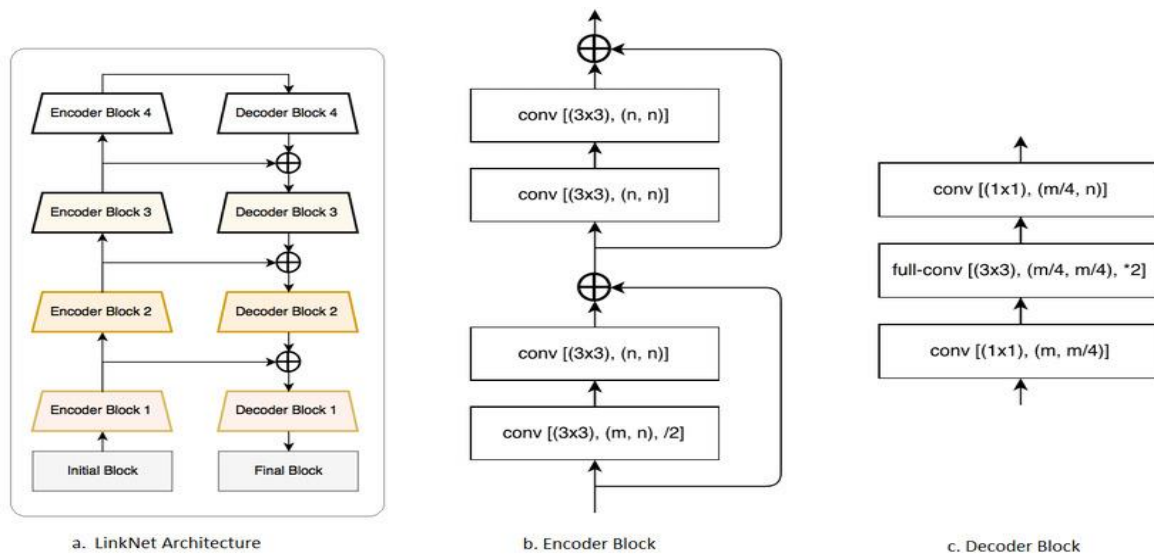


**Figure. 5** (a) LinkNet architecture, (b) convolutional modules in encoder-block, (c) convolutional modules in decoder-block.

LinkNet architecture consists of 4 main processes (Figure 5); "Initial Block", "Decoder Block", "Encoder Block" and "Final Block". The initial block represents the nodule images in which the images are introduced to the system, and the final block represents the predicted nodule images. The number of encoder block and decoder block is 4, here is the part where nodule images are searched in masked lung tomography images, matches are detected, and transferred to the final block. Encoder and decoder blocks are performed by converting images to different matrix sizes and by feedback. The "conv" command is used to convert to different matrix sizes. In the final block are given in Figure 5, the predicted nodule images.

### III. RESULTS

This study started with lung segmentation, then nodule masks were created by exporting the location data of the nodules marked by the Radiologist. The nodules marked by the radiologist are this studies' target nodules, and with the U-Net and LinkNet models used in this study, the intersection of the nodule templates in the images were determined and the nodules in the tomography images were segmented. As indicated in Table 1, the success rate in the images segmented using the LinkNet model, vgg16 backbone, SDG optimizer in terms of success achieved higher success than the other structures.

**Table 1** Success rates for U-Net and LinkNet architecture

	Model	Backbone	Optimizer	Activation	Image_Size	Batch Size	Train Count	Valid Count	Train IoU	Valid IoU	Epoch	Preprocess	Loss	Model
Study1	U-Net	resnet18	SGD	sigmoid	320	8	274	69	0,49	0,4061	100	yes	negative	final
Study2	U-Net	resnet18	SGD	sigmoid	448	8	274	69	0,49	0,37	100	yes	negative	final
Study3	U-Net	resnet34	SGD	sigmoid	384	8	274	69	0,48	0,46	1000	yes	negative	final
Study4	U-Net	resnet50	SGD	sigmoid	320	8	274	69	0,46	0,35	1000	yes	negative	final
Study5	U-Net	resnet34	SGD	sigmoid	320	8	274	69	0,48	0,47	1000	yes	negative	final
Study6	U-Net	Vgg16	SDG	sigmoid	256	16	274	69	0,79	0,64	100	no	positive	final
Study6	U-Net	Vgg16	SDG	sigmoid	256	16	274	69	0,77	0,65	100	no	positive	best
Study7	U-Net	Vgg16	adam	sigmoid	256	16	274	69	0,76	0,59	100	no	positive	final
Study7	U-Net	Vgg16	adam	sigmoid	256	16	274	69	0,71	0,63	100	no	positive	best
Study8	U-Net	vgg19	adam	sigmoid	256	16	274	69	0,58	0,22	100	no	positive	final
Study8	U-Net	vgg19	adam	sigmoid	256	16	274	69	0,78	0,61	100	no	positive	best
Study9	U-Net	vgg19	SDG	sigmoid	256	16	274	69	0,78	0,63	100	no	positive	final
Study9	U-Net	vgg19	SDG	sigmoid	256	16	274	69	0,78	0,63	100	no	positive	best
Study10	U-Net	ef0	SDG	sigmoid	256	16	274	69	0,72	0,58	100	no	positive	final
Study10	U-Net	ef0	SDG	sigmoid	256	8	274	69	0,65	0,61	100	no	positive	best
Study11	U-Net	ef1	SDG	sigmoid	256	8	274	69	0,62	0,56	150	no	positive	final
Study12	U-Net	ef2	SDG	sigmoid	256	8	274	69	0,31	0,14	150	no	positive	final
Study13	LinkNet	vgg16	SDG	sigmoid	256	8	274	69	0,85	0,64	150	no	positive	final
Study14	LinkNet	vgg16	SDG	sigmoid	320	8	274	69	<b>0,94</b>	<b>0,69</b>	150	no	positive	final
Study14	LinkNet	vgg16	SDG	sigmoid	320	8	274	69	<b>0,92</b>	<b>0,69</b>	150	no	positive	best
Study15	LinkNet	seresnet18	SDG	sigmoid	320	8	274	69	0,87	0,55	150	no	positive	final
Study16	LinkNet	vgg19	SDG	sigmoid	288	10	274	69	0,85	0,64	150	no	positive	final



Table 1 shows the determination of the model with the highest success among the models with 16 different architectures by trying different “Bacbone”, “Optimizer”, “Image Size”, “Batch Size” and “Epoch” methods of the U-Net and LinkNet algorithms used in this study. 274 nodule data were used in the train section and 69 nodule data were used in the validation section. The 14<sup>th</sup> study with the highest success rate actually shows the success of this study.

According to the analysis, many researchers have proposed improved techniques and have achieved excellent results for lung nodule segmentation. When a comparison was carried out, the IoU Score of the model proposed by Tan et al. [17] was 65 %. Lassen et al. [18] proposed their technique and achieved an IoU score of 52%. Ronneberger et al. [14] presented their approach, achieving an IoU score of 62.8 %. Moreover, Wu et al. [19] and Aresta et al. [1] achieved IoU scores of 58 and 55, respectively. IoU (%) performance of nodule segmentation between different approaches is given in Table 2.

*Table 2. IoU (%) Performance of nodule segmentation between different approaches*

<b>Sr. No.</b>	<b>Approach</b>	<b>Nodule Amount</b>	<b>IoU Score(%)</b>	<b>Year</b>
1	Tan et al.	23	65	2013
2	Lassen et al.	19	52	2015
3	Ronneberger et al.	59	62.8	2015
4	Wu et al.	1404	58	2018
5	Aresta et al.	284	55	2019
6	<b><i>This Study</i></b>	<b>343</b>	<b>69</b>	----

The above comparison with existing approaches revealed that the proposed model performs well. The segmented lung images are followed by nodules marked by the radiologist and transformed into images (Figure 6). In the area at the end of the figure, a segmented nodule structure with an IoU score 69% is seen. Figure 6 shows that the shape and location data of the nodules marked by the radiologist match the predicted nodules.

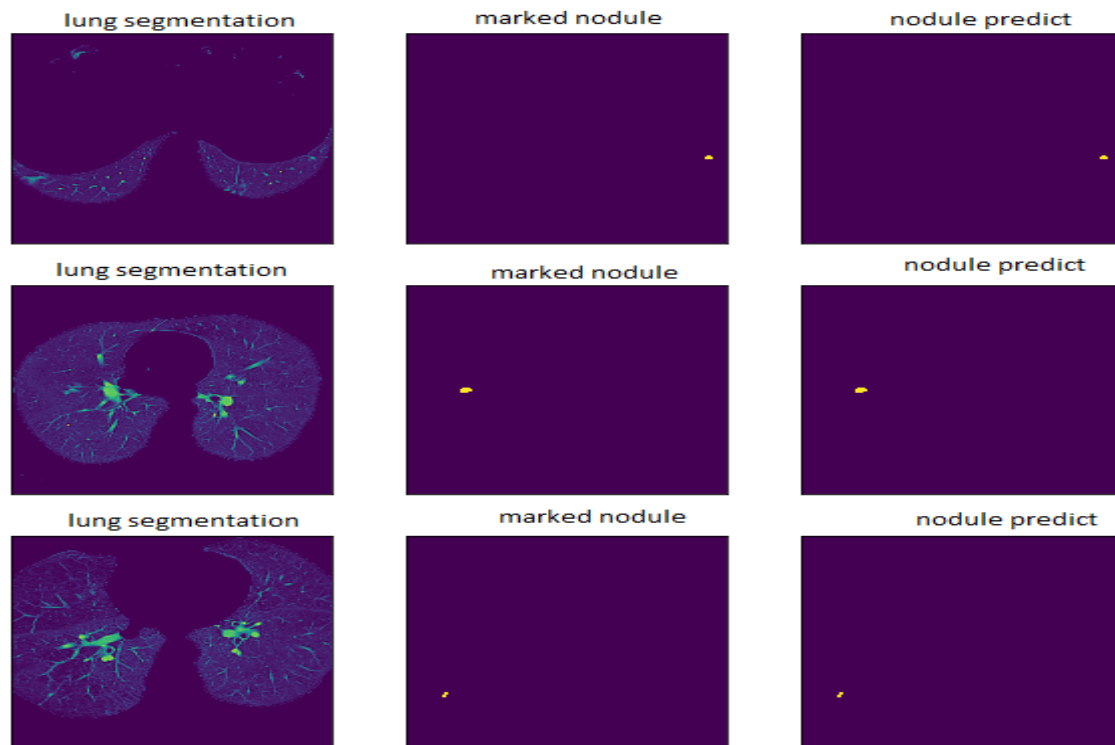


*Fig. 6 Structure of lung nodule detection*

## **IV. CONCLUSION**

In this study, we propose an algorithm that will become a fully automatic system to detect the nodule in the future. Significant gains that will contribute to the literature have been achieved in the study, which is based on increasing the number of specialists who will make the diagnosis and the number of tomography images, and implementing a system that will detect the nodule that a specialist misses and the nodule that others miss and create all nodule masks. In the first stage, a specialist radiologist was used for marking, but with the nodule template database created in different sizes and locations, automatic recommendation was provided instead of the need for a specialist radiologist. Thus, the possibility of missing nodules of all sizes and shapes will be minimized. A total of 110 patients and 343 nodules were used for the study. CT images of 56 male and 54 female patients were used. Firstly, the HU values were determined as threshold values and the lung mask was created with the Otsu method. Afterward, the radiologist marked the nodules and turned them into nodules that were converted to digital location data and then to an image. Using the U-Net and LinkNet models, the intersections of the tomography images were previously determined and the nodules were segmented. This study aims to develop a computer-based diagnostic method with a minimum error rate in hospitals where radiologists work with a high workload. A software infrastructure was created to contribute to the healing process of patients by early diagnosis of nodules missed by the expert radiologist. In this study, as in other studies, a publicly available data set was not used, so that correct classification was achieved by using tomography images taken directly from the hospital and classified, not artificial. When the results of the study were compared with similar studies, it was found to be successful and effective in nodule detection.

Among the important achievements of this study are the study of images of patients in all age groups and the verification of nodules previously marked by a radiologist by a second radiologist. Additionally, examining all parts of the computed tomography image instead of a single part can be stated as an innovation in the literature. Choosing the most successful one among 16 different architectural works instead of a single model and architecture eliminates the limitations of the process and contributes to the diagnosis. The achievements of the study are that detecting nodules with different patterns will increase

the success rate. However, considering the limitations of this study, the time required for the radiologist to mark images for the tomography portion is long. Considering the operations performed, the features of the graphics card to be used for image processing must be very good. Image elimination processes also emerge as the most effective elements that must be followed to achieve good results accurately. According to all these, an important application and library contribution to the literature for the diagnosis of an important disease has been achieved with this study.

## **V. REFERENCES**

- [1] G. Aresta et al., “iW-Net: an automatic and minimalistic interactive lung nodule segmentation deep network,” *Scientific Reports*, vol. 1, no. 1, pp. 1-9, 2019.
- [2] G. A. Borkan, S.G. Gerzof, A.H. Robbins, D.E. Hulst, C.K. Silbert, and J.E. Silbert, “Assessment of abdominal fat content by computed tomography,” *The American Journal of Clinical Nutrition*, vol.36, no.1, pp.172-177, 1982.
- [3] F. Bray, J. Ferlay, I. Soerjomataram, R. L. Siegel, L. A.Torre, and A. Jemal, “Global cancer statistics 2018: GLOBOCAN estimates of incidence and mortality worldwide for 36 cancers in 185 countries,” *CA: a cancer journal for clinicians*, vol. 68, no.6, pp. 394-424, 2018.
- [4] M. Sari and S. Vatansever, “Current trends in the incidence of non-small cell lung cancer in Turkey: lung cancer aging,” *EJMI*, vol.4, no.2, pp.169–172, 2020.
- [5] H. Macmahon et al.,“Guidelines for management of incidental pulmonary nodules detected on CT images: from The Fleischner Society 2017,” *Radiology*, vol.284, no.1, pp. 228-243, 2017.
- [6] M. Javaid, M. Javid, M. Z. U. Rehman, and S. I. A. Shah, “A novel approach to cad system for the detection of lung nodules in CT images,” *Computer Methods and Programs in Biomedicine*, vol. 135, no.2016, pp. 125-139,2016.
- [7] I. W. Harsono, S. Liawatimena, and T. W. Cenggoro, “Lung nodule detection and classification from thorax CT-scan using retinanet with transfer learning,” *Journal of King Saud University-Computer and Information Sciences*, vol.34, no.3, pp.567-577, 2022.
- [8] J. Mukherjee, M. Kar, A. Chakrabarti, and S. Das, “A soft-computing based approach towards automatic detection of pulmonary nodule,” *Biocybernetics and Biomedical Engineering*, vol. 40, no. 3, pp. 1036-1051, 2020.
- [9] A. Gupta, O. Märtens, Y. Le Moullec, and T. Saar, “A tool for lung nodules analysis based on segmentation and morphological operation,” *In 2015 IEEE 9th International Symposium on Intelligent Signal Processing (WISP) Proceedings*, Siena, Italy, 2015, pp. 1-5.
- [10] C. F. J. Kuo et al., “Automatic lung nodule detection system using image processing techniques in computed tomography,” *Biomedical Signal Processing and Control*, vol. 56, no.2020, pp. 101659, 2020.
- [11] C. Zhao, J. Han, Y. Jia, and F. Gou, “Lung nodule detection via 3D U-Net and contextual convolutional neural network,” *In 2018 International Conference on Networking and Network Applications (Nana)*, Xi'an, China, 2018, pp.356-361.
- [12] T. N. Raju, “The nobel chronicles. 1979: allan macleod cormack (b 1924); and sir godfrey newbold hounsfield (B 1919),” *Lancet (London, England)*, vol. 354, no. 9190, pp. 1653,1999.

- [13] W. Xue-guang, C. Shu-hong” An improved image segmentation algorithm based on two-dimensional Otsu method,” *Information Sciences Letters*, vol.1, no.3, pp. 2, 2012.
- [14] A. Rosset, L. Spadola, and O. Ratib, “Osirix: an open-source software for navigating in multidimensional DICOM images,” *Journal of Digital Imaging*, vol.17, no.3, pp. 205-216, 2004.
- [15] O. Ronneberger, P. Fischer, and T. Brox, “U-Net: convolutional networks for biomedical image segmentation,” *In International Conference On Medical Image Computing and Computer-Assisted Intervention*, Munich, Germany, 2015, pp.1-8.
- [16] A. Chaurasia and E. Culurciello,” Linknet: Exploiting encoder representations for efficient semantic segmentation,” *In 2017 IEEE Visual Communications and Image Processing (VCIP)*, St. Petersburg, FL, USA, 2017, pp.1-4.
- [17] Y. Tan, L. H. Schwartz, and B. Zhao, ”Segmentation of lung lesions on CT scans using watershed, active contours, and Markov random field” *Medical Physics*, vol. 40, no.4, pp. 043502, 2013.
- [18] C. Lassen, C. Jacobs, J. M. Kuhnigk, B. Van Ginneken, and E. M. Van Rikxoort,”Robust semi-automatic segmentation of pulmonary subsolid nodules in chest computed tomography scans,”*Physics in Medicine & Biology*, vol.60, no.3, pp. 1307, 2015.
- [19] B. Wu, Z. Zhou, J. Wang, and Y. Wang,” Joint learning for pulmonary nodule segmentation, attributes and malignancy prediction,” *In 2018 IEEE 15th International Symposium on Biomedical Imaging (ISBI 2018)*, Washington, USA, 2018, pp.1109-1113.